PAPER

Winding in non-Hermitian systems

IOP Publishing Journal of Physics A: Mathematical and Theoretical

J. Phys. A: Math. Theor. **51** (2018) 055201 (16pp) https://doi.org/10.1088/1751-8121/aa9faf

Winding in non-Hermitian systems

Stella T Schindler and Carl M Bender[1]

Department of Physics, Washington University, St. Louis, MO 63130, United States of America

E-mail: cmb@wustl.edu

Received 14 April 2017, revised 28 November 2017
Accepted for publication 7 December 2017
Published 28 December 2017

Abstract

This paper extends the property of interlacing of the zeros of eigenfunctions in Hermitian systems to the topological property of winding number in non-Hermitian systems. Just as the number of nodes of each eigenfunction in a self-adjoint Sturm–Liouville problem are well-ordered, so too are the winding numbers of each eigenfunction of Hermitian and of unbroken $\mathcal{PT}$-symmetric potentials. Varying a system back and forth past an exceptional point changes the windings of its eigenfunctions in a specific manner. Nonlinear, higher-dimensional, and general non-Hermitian systems also exhibit manifestations of these characteristics.

Keywords: interlacing, PT symmetry, winding

(Some figures may appear in colour only in the online journal)

1. Introduction

Recent research and experiments on non-Hermitian systems have unearthed a trove of new physical phenomena and potential applications [1–6]. A deeper understanding of the fundamental mathematical underpinnings of these systems is necessary to help drive further experimental advances. In this theoretical paper, we explore the structure of eigenfunctions of non-Hermitian Hamiltonians. We believe that our findings will help elucidate aspects of wave propagation in non-Hermitian systems, such as those describing optical waveguides.

Hamiltonians respecting $\mathcal{PT}$*-symmetry* form a noteworthy class of non-Hermitian systems. A $\mathcal{PT}$-symmetric potential $V(x)$ satisfies $V(x) = V^*(-x)$, where * represents complex conjugation. The positive and negative imaginary parts of a non-Hermitian potential represent gain and loss, respectively. Thus, a $\mathcal{PT}$-symmetric system has a net-zero, *balanced* energy exchange with its surroundings [7].

In quantum mechanics, it is often said that a Hamiltonian H must be Hermitian, $H = H^\dagger$, to have all real eigenvalues. This is false: a non-Hermitian system with unbroken $\mathcal{PT}$ symmetry

[1] Author to whom any correspondence should be addressed.

also has an entirely real spectrum [8]. Furthermore, one can construct an inner-product under which the eigenfunctions of a $\mathcal{PT}$-symmetric Hamiltonian have positive norms and exhibit unitary time evolution. Thus, such Hamiltonians define physical quantum theories [7].

We may view the study of $\mathcal{PT}$-symmetric Hamiltonians as a stepping stone from the comparatively simple analysis of real systems towards an understanding of full-fledged non-Hermiticity. Specifically, $\mathcal{PT}$ spectral reality and unitarity suggest that other hallmark features of Hermitian Hamiltonians might also have $\mathcal{PT}$ analogues that only fully break down with loss of symmetry.

In this paper, we describe a topological extension of the Hermitian property of *interlacing of eigenfunctions*. Interlacing means that between any two consecutive *nodes*, or zeros, of an eigenfunction lies exactly one node of the next-higher-energy eigenfunction [9]. This is strongly associated with the completeness of the eigenfunctions. $\mathcal{PT}$-symmetric eigenfunctions also comprise a complete set [10]; however, no $\mathcal{PT}$ counterpart of Hermitian interlacing has yet been defined. (There does exist an observation of analogous behavior of eigenfunction zeros in the complex plane, but it is only a numerical exploration [11].)

We show that a slight $\mathcal{PT}$-symmetric perturbation of a Hermitian eigenfunction induces looping about the x-axis of a complex-valued, nodeless curve. The nature of the loops, or *winds*, has a precise mathematical description.

The *winding number* of a function $\psi(x)$ is the amount by which it rotates about the x-axis in the space $[x, \mathrm{Re}\,\psi(x), \mathrm{Im}\,\psi(x)]$. If we take the polar decomposition of the function $\psi(x) = r(x)\mathrm{e}^{\mathrm{i}\theta(x)}$ with $r(x)$ and $\theta(x)$ real-valued, then we can define the winding W as

$$W[\psi(x)] \equiv \int \mathrm{d}x\, \theta_x(x). \tag{1}$$

Throughout this paper we express the winding number as *the overall angle in radians traversed by a function*.

In the introductory section of this paper, we first show that the eigenfunctions of unbroken $\mathcal{PT}$-symmetric Hamiltonians wind and that their winding numbers $W_n = W[\psi_n(x)]$ are distinct and well-ordered. We view Hermitian interlacing as a degenerate signature of this well-ordered winding. To illustrate, we begin with the canonical examples of quantum theory and advance towards nontrivial results. For the remainder of the paper, we discuss more complicated systems, such as those with broken symmetries, and briefly highlight relevance to physical applications.

1.1. Square-well potential

We consider first the square-well potential

$$V(x) = \begin{cases} 0 & (0 \leqslant x \leqslant \pi), \\ \infty & \text{otherwise}, \end{cases}$$

with imposed boundary conditions $\psi_n(0) = \psi_n(\pi) = 0$. The eigenfunctions of this system are $\psi_n(x) = \sin(nx)$ with corresponding eigenvalues $\lambda_n = n^2$. These eigenfunctions exhibit Hermitian interlacing because the $n-1$ nodes of $\psi_n(x)$ lie at $x = \frac{\pi}{n}, \frac{2\pi}{n}, \ldots, \frac{(n-1)\pi}{n}$. (Boundary points are not nodes [9].)

We extend these eigenfunctions into the complex plane:

$$\psi_n(x) = \sin(nx) \;\rightarrow\; \psi_n(z) = \sin(nz).$$

We may now traverse a *complex* path to get from one boundary point to the other. This path is parametrized as $[t, f(t)]$, where the real parameter t lies in the interval $(0, \pi)$

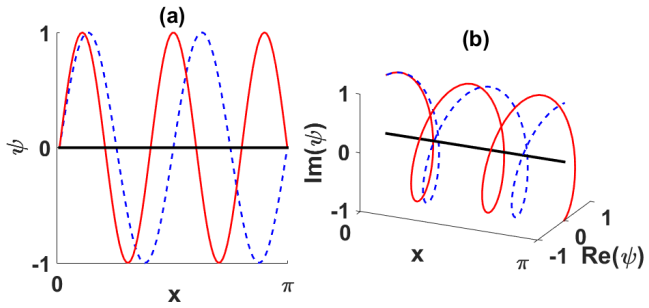

Figure 1. (a) Interlacing of eigenfunctions of the Hermitian square-well potential on the real axis. Between any two zeros of $\psi_4(x) = \sin 4x$ (red solid curve) lies exactly one zero of $\psi_3(x) = \sin 3x$ (blue dashed curve). (b) Winding of eigenfunctions of the square-well potential in the complex plane: $\psi_4(x) = \mathrm{e}^{4\mathrm{i}x}$ (red solid curve) and $\psi_3(x) = \mathrm{e}^{3\mathrm{i}x}$ (blue dashed curve) both wind not only about the x-axis but also about one another.

and $f(t)$ is complex valued. We thus may write $f(t) = f_R(t) + \mathrm{i}\epsilon f_I(t)$, where ϵ is a real parameter and $f_R(t)$ and $f_I(t)$ are real-valued smooth functions. Along this new path the eigenfunctions are

$$\psi_n(t) = \sin[nf_R(t)]\,\cosh[\epsilon n f_I(t)] + \mathrm{i}\,\cos[nf_R(t)]\,\sinh[\epsilon n f_I(t)].$$

The hyperbolic sine and cosine functions are real-valued, positive, and monotonically increasing on the positive-real numbers. Thus, $\psi_n(t)$ winds in a single direction about the axis much like a helix, albeit not always at a uniform distance from the x-axis. These helical eigenfunctions have distinct and well-ordered winding numbers $W_n = n\pi$. In the limit $\epsilon \to 0$ this winding flattens out onto the real axis and reduces to the usual Hermitian interlacing pattern (see figure 1). Note that in addition to winding about the x-axis, the eigenfunctions $\mathrm{e}^{\mathrm{i}nx}$ and $\mathrm{e}^{\mathrm{i}(n+1)x}$ also *wind about each other* exactly n times [13][2].

Let us reconsider the square-well potential in an alternative manner. Before we impose boundary conditions, the extended eigenfunctions are

$$\psi_n(x) = c_1 \sin(nx) + \mathrm{i}c_2 \cos(nx).$$

By choosing $c_1 = c_2 = 1$, we can calculate exactly the winding of

$$\psi_n(x) = \sin(nx) + \mathrm{i}\cos(nx) = \mathrm{i}\mathrm{e}^{-\mathrm{i}nx}$$

to be $n\pi$, as the eigenfunctions are perfect helices about the x-axis. Other choices $c_1 \neq c_2$ correspond to helices with elliptical (not circular) projections onto the plane $[\mathrm{Re}\,\psi_n(x), \mathrm{Im}\,\psi_n(x)]$ with the same overall winding number. The eccentricity of the ellipse grows as $c_2 \to 0$ but the winding number remains the same. The degenerate limiting case $c_2 = 0$ corresponding to the boundary condition $\psi(0) = \psi(\pi) = 0$ projects onto a line, which reduces to the flat, Hermitian case of $\psi_n(x) = c_1 \sin(nx)$.

The prior two explanations are fundamentally the same because the analytic extension $\sin(nx) \to \sin(nz)$ may be expressed as $\sin(nx + \mathrm{i}ny) = \sin(nx)\cosh(ny) + \mathrm{i}\cos(nx)\sinh(ny)$.

[2] The winding of consecutive square-well eigenfunctions about one another bears resemblance to braids and knots. The appearance of these properties in Hermitian systems becomes intuitive from section 1.1. It is of interest to study the property of braiding in non-Hermitian systems and in particular the effect of symmetry-breaking exceptional points on braiding. It is possible that, just as in moving from the real line to the complex plane one loses the property of ordering numbers, one also loses braiding in non-Hermitian systems.

Curves along which $\mathrm{Im}\, z = y_0$ remains constant correspond precisely to linear combinations of the linearly independent solutions $\sin(nx)$ and $\cos(nx)$, albeit with imposed boundary condition $\psi_n(iy_0) = \psi_n(\pi + \mathrm{i}y_0) = \mathrm{i}\,\sinh y_0$.

1.2. Linear system on a finite domain

To explain and generalize the results for the square-well potential we employ two standard theorems on Hermitian *Sturm–Liouville* problems; namely, differential equations of the general form

$$-Eh(x)\psi(x) = \frac{\mathrm{d}}{\mathrm{d}x}\left[f(x)\frac{\mathrm{d}\psi(x)}{\mathrm{d}x}\right] + g(x)\psi(x).$$

We first note that for a rising potential $V(x)$ the Schrödinger equation

$$\mathrm{i}\psi_t(x,t) = -\psi_{xx}(x,t) + V(x)\psi(x,t)$$

possesses a countably infinite number of stationary solutions $\psi_n(x,t) = \psi_n(x)\mathrm{e}^{-\mathrm{i}E_n t}$, $E_n \in \mathbb{R}$, governed by the time-independent Schrödinger eigenvalue equation

$$E\psi(x) = -\psi_{xx}(x) + V(x)\psi(x), \tag{2}$$

which is in Sturm–Liouville form. The *Sturm–Picone Comparison Theorem* in our case is equivalent to the statement that the eigenfunctions of a Hermitian Hamiltonian interlace. The *Sturm Separation Theorem* considers any two linearly independent solutions $u(x)$ and $v(x)$ corresponding to the same eigenvalue of a Sturm–Liouville problem without boundary conditions imposed. The theorem states that $u(x)$ and $v(x)$ must have the same number of nodes and that $u(x)$ and $v(x)$ exhibit a type of interlacing. Between any two consecutive nodes of $u(x)$ lies exactly one node of $v(x)$ and vice versa [9].

For Hermitian Hamiltonians, we may always take $u(x)$ and $v(x)$ to be real valued. The Sturm Separation Theorem implies that all extended Hermitian eigenfunctions $\psi_n(x) = c_1 u_n(x) + \mathrm{i}c_2 v_n(x)$ with $c_1, c_2 \in \mathbb{R}$ exhibit winding. Furthermore, adjusting the boundary conditions to approach the limit $c_2 \to 0$ corresponds to approaching the proper eigenfunctions $\psi_n(x)$ that exhibit degenerate winding number and Hermitian interlacing.

1.3. Harmonic oscillator potential

Sturm–Liouville problems with boundary conditions at infinity also exhibit distinct and well-ordered windings. For example, consider the harmonic-oscillator potential $V(x) = x^2$ with eigenfunctions that vanish at $\pm\infty$. The eigenfunctions of this problem are

$$\psi_n(x) = H_n(x)\mathrm{e}^{-x^2/2},$$

where $H_n(x)$ is the nth Hermite polynomial. We again perform a complex extension and find the winding numbers of the extended eigenfunctions

$$\psi_n(x + \mathrm{i}\epsilon) = H_n(x + \mathrm{i}\epsilon)\mathrm{e}^{-(x+\mathrm{i}\epsilon)^2/2}.$$

For $\epsilon \neq 0$, the system corresponds to the unbroken $\mathcal{PT}$-symmetric shifted harmonic oscillator problem $V(x) = (x + \mathrm{i}\epsilon)^2$ [14]. The term $\mathrm{e}^{(\epsilon^2 - x^2)/2}$ does not contribute to the winding of the eigenfunctions. The $\mathrm{e}^{\mathrm{i}\epsilon x}$ term adds to each eigenfunction an infinite number of winds about the x-axis, but these winds are independent of n. The distinctness of the eigenfunction windings arises from the other term; that is, the Hermite polynomials:

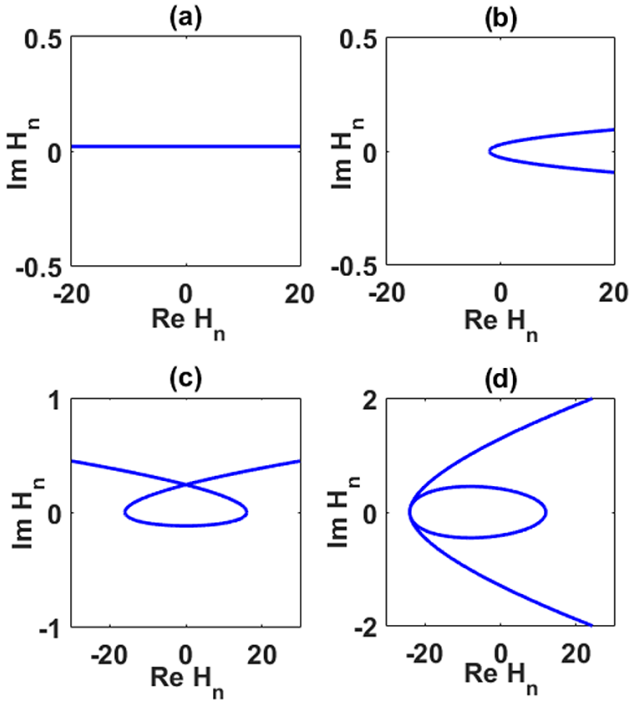

Figure 2. (a)–(d) Projections of the complex Hermite polynomials $H_n(x+\mathrm{i}\epsilon)$ onto the plane $(\mathrm{Re}\,H_n,\ \mathrm{Im}\,H_n)$ for fixed $\epsilon = 0.001$ and $n = 1, 2, 3, 4$. Each additional half-loop traversed by a curve corresponds to an additional winding of π traversed by the eigenfunctions of the $\mathcal{PT}$-symmetric harmonic oscillator.

$$
\begin{aligned}
H_0(x+\mathrm{i}\epsilon) &= 1,\\
H_1(x+\mathrm{i}\epsilon) &= 2x+2\mathrm{i}\epsilon,\\
H_2(x+\mathrm{i}\epsilon) &= 4x^2-4\epsilon^2-2+4\mathrm{i}\epsilon x,\\
H_3(x+\mathrm{i}\epsilon) &= x^3-3\epsilon^2x-12x-\mathrm{i}(12\epsilon-3\epsilon x^2+3\epsilon^3).
\end{aligned}
$$

By integrating, we find that $H_n(x+\mathrm{i}\epsilon)$ winds through an angle of $n\pi$ about the x-axis. Therefore, the infinities cancel; that is, $W[\psi_n(x)]-W[\psi_m(x)] = (m-n)\pi$. The eigenfunctions are well-ordered even though the total number of winds is infinite. We plot the projections $(\mathrm{Re}\,H_n, \mathrm{Im}\,H_n)$ of the first few Hermite polynomials in figure 2. Note that in the Hermitian limit $\epsilon \to 0$, the infinite winding term $\mathrm{e}^{\mathrm{i}\epsilon x}$ completely disappears from the eigenfunctions. Again we observe the degenerate and finite signature of winding; namely, interlacing on the real axis.

1.4. $\mathcal{PT}$-symmetric cubic potential

Next, we consider the $\mathcal{PT}$-symmetric potential $V(x) = \mathrm{i}x^3$ on a *finite* domain with eigenfunctions that are required to vanish at $x = \pm L$. This equation is not analytically soluble, so we perform a WKB analysis of the time-independent Schrödinger equation

$$-\epsilon^2\psi''(x) = [E-V(x)]\psi(x)$$

in order to determine the behavior of high-energy eigenfunctions. We treat the parameter ϵ as small, and thus the WKB approximation to the nth eigenfunction for $n \gg 1$ is

$$\psi_n(x) \sim \frac{C_\pm}{[E_n - V(x)]^{1/4}} \exp\left[\pm\frac{i}{\epsilon}\int^x \mathrm{d}s\sqrt{E_n - V(s)}\right].$$

Setting $\psi(-L) = 0$ implies that

$$\psi_n(x) \sim \frac{C}{[E_n - V(x)]^{1/4}} \sin\left[\frac{1}{\epsilon}\int_{-L}^x \mathrm{d}s\sqrt{E_n - V(s)}\right]. \tag{3}$$

We further impose $\psi(L) = 0$ and find that

$$n\pi \sim \frac{1}{\epsilon}\int_{-L}^{L} \mathrm{d}s\sqrt{E_n - V(s)}.$$

Hence, for large E_n, we see that

$$E_n \sim \frac{n^2\pi^2\epsilon^2}{4L^2}. \tag{4}$$

We now substitute (4) into (3). For large n we may set $\epsilon = 1$, and we get

$$\psi_n(x) \sim C\left[\frac{n^2\pi^2}{4L^2} - V(x)\right]^{-1/4} \sin\int_{-L}^x \mathrm{d}s\sqrt{\frac{n^2\pi^2}{4L^2} - V(s)}.$$

The term $C\left[n^2\pi^2/(4L^2) - V(x)\right]^{-1/4}$ contributes the same amount of winding for each eigenfunction. Thus, we need only consider the effect of the sine term. Substituting $V(s) = \mathrm{i}s^3$ and making a binomial approximation to the square root, we find that

$$\sin\int_{-L}^x \mathrm{d}s\sqrt{\frac{n^2\pi^2}{4L^2} - \mathrm{i}s^3} \sim \sin\left(\frac{n\pi x}{2L}\right)\cosh\left[\frac{n\pi(L^4 - x^4)}{16L}\right] - \cos\left(\frac{n\pi x}{2L}\right)\sinh\left[\frac{n\pi(L^4 - x^4)}{16L}\right].$$

Since $\sinh y \sim \cosh y$ for large positive y, we get

$$\sin\int_{-L}^x \mathrm{d}s\sqrt{\frac{n^2\pi^2}{4L^2} - \mathrm{i}s^3} \sim D_n \exp\left[\frac{-\mathrm{i}n\pi x}{2L}\right],$$

which has winding number $n\pi$ on $-L \leqslant x \leqslant L$.

1.5. General remarks

For many non-Hermitian potentials, as long as L remains finite, the high-energy eigenfunctions possess finite and distinct winding numbers. If L is infinite, the eigenfunctions may possess infinite but still well-ordered winding numbers. To understand this behavior we consider the complex extensions of the eigenfunctions $\psi_n(x) \to \psi_n(z)$. There exists a complex contour $\mathcal{C}_1$ between the turning points of $\psi_n(z)$ on which $\psi_n(z)$ is entirely real. Furthermore, $\psi_n(z)$ has exactly n nodes on this path. However, on the other sides of the turning points there exist *constant-phase* contours $\mathcal{C}_2$ and $\mathcal{C}_3$ from the location of the turning point out to infinity on which the eigenfunction possesses a constant angular argument and never vanishes [11, 12]. Thus, eigenfunctions defined along the curve $\mathcal{C} = \mathcal{C}_1 + \mathcal{C}_2 + \mathcal{C}_3$ possess a Hermitian-like degenerate winding $n\pi$. Continuously deforming $\mathcal{C}$ to the real axis pulls the eigenfunction out

of the well-behaved-phase region into an oscillatory region and induces infinite but distinct windings, like the $\mathcal{PT}$-symmetric shifted harmonic oscillator discussed in section 1.3.

The windings of the eigenfunctions also need not be consecutive multiples of π. It is possible to construct a complete set of *exceptional orthogonal polynomials* which lack polynomials of a finite number of chosen degrees. These polynomials (when multiplied by the appropriate weight function) may correspond to the eigenfunctions of a Hamiltonian system [15]. The degree of a polynomial corresponds to its winding number. An orthogonality weight contributes equally to the winding of each function. Thus, it may be possible to observe winding skips of greater than π between two consecutive eigenfunctions. A family of quasi-orthogonal polynomials may also exhibit interesting zero behaviors in the complex plane [16]. These functions could serve as an additional way to probe the relationship between complex zero locations and winding on the real line. Studies of winding in these simple models as well as other more exotic sets of functions could offer valuable insights.

We have explained how the phase angles $\theta_n(x)$ of unbroken $\mathcal{PT}$-symmetric eigenfunctions $\psi_n(x)$ depend locally on x. We now explore broader classes of systems, including those with broken symmetry. To do this, we discuss the winding of eigenfunctions in a global sense: as functions of a parametrized Hamiltonian $H(x,\epsilon)$.

This paper is organized as follows. We describe the dependence of eigenfunction winding on the degree of symmetry breaking present in linear, nonlinear, and time-dependent Schrödinger equations in section 2. In section 3 we illustrate how winding manifests in much broader classes of differential equations by perturbing into the complex plane a previously studied nonlinear differential equation problem exhibiting ordered oscillations. We offer concluding remarks in section 4.

2. Broken symmetry

A theorem of Sturm states that the zeros of the real-valued eigenfunctions of Hermitian Hamiltonians interlace. In section 1, we demonstrated that this interlacing is a degenerate, limiting signature of the more general phenomenon of eigenfunction winding in the complex plane. We may observe this winding by integrating the differential equation from one boundary point to the other along a path through the complex plane instead of along the real axis. We may also see this winding by perturbing the boundary conditions on the eigenfunction into the complex plane and then taking the limit as the boundary conditions approach the real axis. We emphasize that unbroken $\mathcal{PT}$-symmetric Hamiltonians exhibit the same winding behavior as Hermitian Hamiltonians.

To describe the full class of $\mathcal{PT}$-symmetric Hamiltonians, including systems with broken symmetry, we insert a parameter ϵ into a $\mathcal{PT}$-symmetric potential $V(x) \to V(x;\epsilon)$. By varying ϵ, we may vary the degree of symmetry or symmetry-breaking present in the system. By convention, we insert ϵ in such a way that $V(x;0)$ is Hermitian. A value of ϵ at which the Hamiltonian operator is *singular*, that is, at which at least one pair of eigenfunctions possesses the same eigenvalue, is called an *exceptional point* [17, 18]. Past an exceptional point (in a region of *broken* $\mathcal{PT}$ symmetry) one or more pairs of eigenvalues are complex conjugates and their corresponding eigenfunctions satisfy $\psi_1(x) = c\,\psi_2^*(-x)$, where c is some complex constant. We define the *degree of symmetry breaking* of a Hamiltonian $H(x,\epsilon_0)$ as the number of its eigenvalues that are paired or complex-valued. This degree corresponds to the number of non-well-ordered eigenfunctions in the system.

When we vary ϵ in a region of unbroken $\mathcal{PT}$ symmetry, the eigenfunctions of $\mathcal{H}(x,\epsilon)$ deform continuously, with two exceptions: (i) the flattening of infinite winding on an infinite domain at the point of Hermiticity (like the harmonic oscillator) or (ii) the formation of singularity in the operator perhaps due to the breaking of a symmetry other than $\mathcal{PT}$ symmetry. We now explain the general phenomenon of well-ordered windings as a consequence of the absence of eigenfunction nodes on the real axis in a region of unbroken symmetry [11].

Why do eigenfunctions lack nodes on the real axis? As long as the value of ϵ does not correspond to an exceptional point, the operator $\mathcal{H}(x,\epsilon)$ is nonsingular. Thus, for a fixed nonexceptional value of ϵ, we may take a polar decomposition of any eigenfunction $\psi(x) = r(x)\mathrm{e}^{\mathrm{i}\theta(x)}$. If $\psi(x)$ vanishes at some point $x = x_0$, then $r(x_0) = 0$. Furthermore, $r(x)$ is always nonnegative, so $r_x(x_0) = 0$. Thus, $\psi_x(x_0) = [r_x(x_0) + \mathrm{i}r(x_0)\theta_x(x_0)]\mathrm{e}^{\mathrm{i}\theta(x_0)} = 0$. The vanishing of $\psi(x)$ and $\psi_x(x)$ at $x = x_0$ implies that all derivatives of $\psi(x)$ vanish at $x = x_0$ because $\psi(x)$ obeys the Schrödinger equation. If all derivatives of an analytic function are zero at a point, then that function is constant. But $\psi(x) = 0$ contradicts the assumption that $\psi(x)$ is an eigenfunction. Thus, $\psi(x)$ does not vanish on the real axis.

Because eigenfunctions of unbroken $\mathcal{PT}$-symmetric operators are nodeless, their windings do not exhibit any sudden discontinuities as we vary ϵ. Thus, the windings of eigenfunctions vary continuously in the region of unbroken $\mathcal{PT}$ symmetry. This in turn leads to the winding-number-based ordering of eigenfunctions.

What happens at an exceptional point (where the operator is singular)? As ϵ approaches an exceptional point, a pair of solutions begins to coalesce. At the exceptional point, these two eigenfunctions are identical and therefore possess the same winding number. Past the exceptional point, the solutions ψ_1 and ψ_2 are $\mathcal{PT}$ conjugates, so they still have the same winding number: $W[\psi_1(x)] = W[\psi_2(x)]$.

The ϵ dependence of eigenfunctions with complex eigenvalue is distinct from that of eigenfunctions with real eigenvalue. As we parametrically pass through an exceptional point, the windings of the eigenfunctions undisturbed by the crossing with real corresponding eigenvalue remain ordered with respect to one another in the same manner as prior to the crossing. However, eigenfunctions having complex eigenvalues need not respect that order. That is, a higher degree of symmetry breaking corresponds to well-ordering by winding of fewer eigenfunctions.

The eigenfunctions of a non-Hermitian Hamiltonian $\mathcal{H}(x;\epsilon)$ that lacks symmetry do not necessarily exhibit any of these characteristics (see figure 3). Due to the lack of consistency in singularity formation in $\mathcal{H}(x;\epsilon)$ with respect to the parameter ϵ, eigenvalues may develop multiplicities or become complex in a nonuniform fashion. Eigenfunctions may also develop nodes unsystematically and do not shift windings in a prescribed manner past a singular point. Thus, deformations of non-Hermitian Hamiltonians do not have to maintain strict eigenvalue-based order or well-predicted pairings of winding numbers. We remark that these properties extend to higher-dimensional systems[3]. Note that it is also of interest to find out the extent to which the topological properties of a set of eigenfunctions could inform us about the nature of their corresponding Hamiltonian operator.

[3] Winding is not just a property of the eigenfunctions of one-dimensional systems. The solutions to a complex N-dimensional Schrödinger equation $E\psi(\vec{x}) = -\nabla^2\psi(\vec{x}) + V(\vec{x})\psi(\vec{x})$ are N-dimensional manifolds looping about the x_1-plane in an (N + 2)-dimensional space. As in section 2 one can show that $\mathcal{PT}$-symmetric potentials may not possess nodes except at an exceptional point. Thus, we begin to visualize intuitively an N-dimensional extension of winding based on how many times the manifold wraps around its domain, that is, the *topological degree* of the mapping. Simple examples of this include the N-dimensional square-well and N-dimensional harmonic oscillator potentials, whose eigenfunctions are merely products of N one-dimensional square-well and harmonic oscillator eigenfunctions, respectively. Multidimensional systems with exceptional points will be explored in future work.

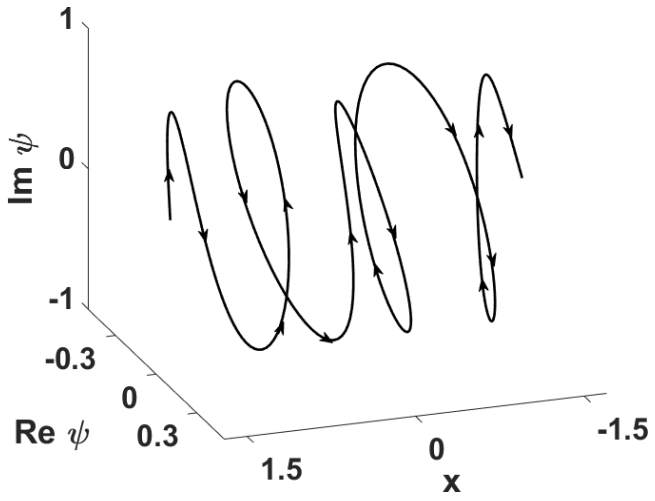

Figure 3. Ninth eigenfunction of the non-Hermitian potential $V(x) = x\sin x + \mathrm{i}\epsilon\cos(3x)$ for $\epsilon = 20$ plotted as the curve $[x, \mathrm{Re}\,\psi(x), \mathrm{Im}\,\psi(x)]$ on the interval $-\pi/2 \leqslant x < \pi/2$. Observe that eigenfunctions of an arbitrary non-Hermitian system need not behave in as orderly a fashion as eigenfunctions of a Hermitian or $\mathcal{PT}$-symmetric system. As we increase ϵ in $V(x)$ from 0–20, the system passes through singularities, and thus eigenfunction windings change in an irregular manner compared to that of a $\mathcal{PT}$-symmetric system. The plotted eigenfunction has winding number *zero* because the phase loops twice about the x-axis in one direction, turns around, and then makes two loops in the opposite direction. Thus, in terms of phase angle, $W[\psi_9(x)] = \int_{\pi/2}^{\pi/2}\theta_x(x)\mathrm{d}x = 0$.

The statements above appear to hold for all potentials. However, the extra constraints that periodicity places on a system lead to noticeable distinctions from their nonperiodic counterparts. We present two examples to highlight these differences. We then examine how similar properties appear even when the system is nonlinear.

2.1. Nonperiodic potential

Consider first the linear Schrödinger eigenvalue equation (2) with the nonperiodic $\mathcal{PT}$-symmetric potential

$$V(x) = 4 - 4\mathrm{i}\epsilon x$$

on the finite interval $[-\pi/2, \pi/2]$. We impose homogeneous boundary conditions at the endpoints. As predicted, the eigenfunction windings deform smoothly and continuously in the region between two exceptional points. At an exceptional point, the winding numbers of two eigenfunctions merge. The exceptional point is the sole point of nonsmooth variation of winding numbers; the derivative $\frac{\mathrm{d}W_n}{\mathrm{d}t}$ may be different on either side of the transition. Beyond an exceptional point, however, these winding numbers vary smoothly once more and in tandem. That is, nonsmooth winding deformation occurs only at an exceptional point and only for the specific eigenfunctions with coalesced eigenvalues. We plot the phase of the eigenfunctions at each (x, ϵ) value in figure 4.

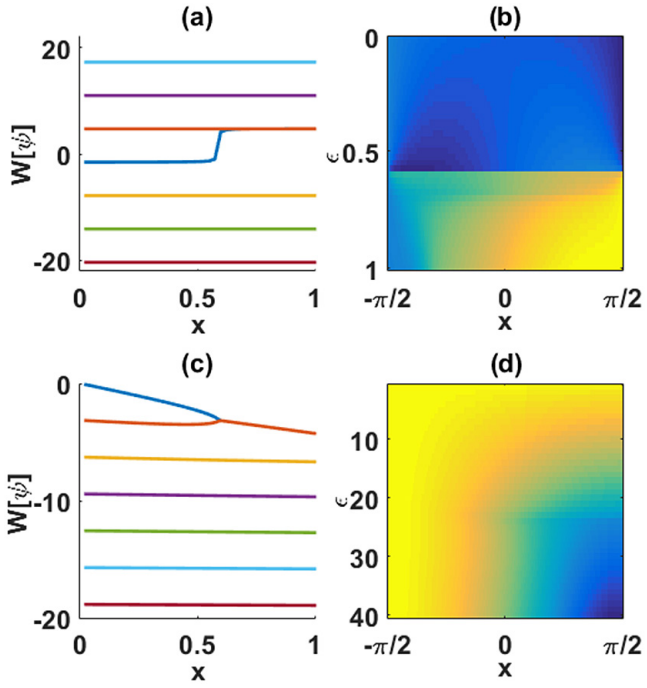

Figure 4. Dependence of eigenfunction winding on the parameter ϵ for the nonperiodic potential $V(x) = 4 - 4\mathrm{i}\epsilon x$ (panel (a)) and the periodic potential $V(x) = 4\cos^2 x + 4\mathrm{i}\sin(2x)$ (panel (c)). The corresponding phase angles $\theta(x, \epsilon)$ of the first eigenfunction of each potential for a range of (x, ϵ) are shown in (b) and (d). Note the sharp jump discontinuity in both eigenvalue magnitude and eigenfunction phase-angles function at an exceptional point (panel (b)), compared to the continuous dependence on ϵ for the nonperiodic potential (panel (d)).

2.2. Periodic potential

The eigenfunctions of a $\mathcal{PT}$-symmetric periodic potential, unlike those of a nonperiodic potential, always possess winding numbers that are equivalent modulo 2π. This property is due to Bloch's theorem, which states that solutions to a Schrödinger equation with a periodic potential take the form

$$\psi_n(x) = u_n(x)\mathrm{e}^{\mathrm{i}kx},$$

where $-\pi \leqslant k < \pi$ is a chosen Bloch wavenumber. Thus, any change in winding must occur as a discontinuous jump. As we approach an exceptional point the behavior of the eigenfunctions is not immediately apparent.

Thus, let us examine the complex phase at every point of the wave. We consider the potential

$$V(x) = 4\cos^2 x + 4\mathrm{i}\epsilon\sin(2x), \tag{5}$$

which was studied in [19]. We first find the eigenfunctions for $k \neq 0$. Figure 4 shows that in the region of unbroken symmetry the eigenfunctions have winding numbers $W_{2n} = -W_{2n+1}$. The approach towards an exceptional point is marked not only by the formation of a sharp cusp in eigenfunction magnitude but also by the corresponding formation of a jump discontinuity in eigenfunction phase. The eigenfunction tries to complete a full loop about the x-axis within

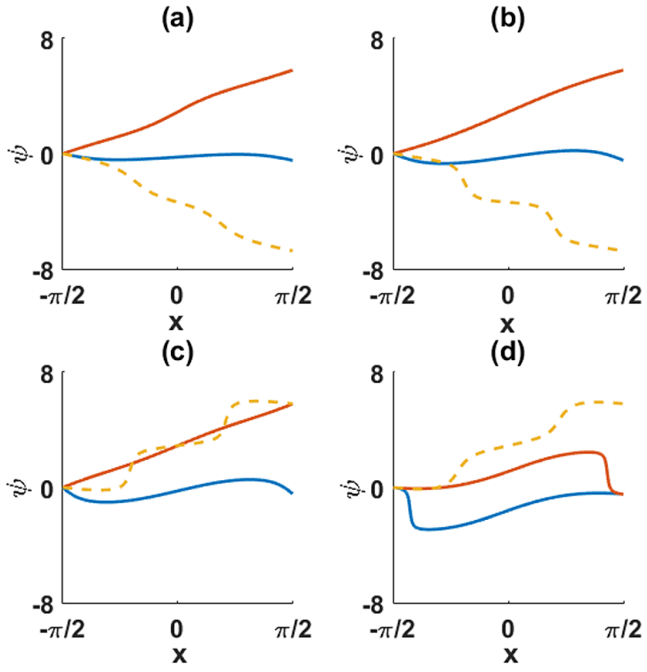

Figure 5. Phase angle at every point of the first three eigenfunctions (solid blue, solid red, dashed yellow) of the Schrödinger equation with additive cubic ($|\psi|^2\psi$) nonlinearity and potential $V(x) = 4\cos^2 x + 4\mathrm{i}\epsilon\sin(2x)$ for $\epsilon = 0.25,\ 0.50,\ 0.75, 1.00$ in panels (a)–(d). All of the eigenfunctions have real corresponding eigenvalue except for the first and second eigenfunctions, which have become $\mathcal{PT}$ conjugates (panel (d)). Note the approach towards a jump discontinuity in phase angle near a singular point. The third eigenfunction is always associated with a real eigenvalue, and the jump in its winding for $\epsilon \in (0.50, 0.75)$ does not occur because of $\mathcal{PT}$ symmetry breaking.

an extremely short distance. As that length reaches zero, the system crosses an exceptional point and the eigenfunction winding jumps. Interestingly, only one eigenfunction of the pair exhibits this type of dependence on ϵ rather than a mutual merging as observed in the nonperiodic case. At $\epsilon = 0.5$, all the bands go complex simultaneously at their edges $k = \pm 1$. At this parameter value, the eigenfunctions have exact solutions in terms of Bessel functions [19]:

$$u(x) = J_k(\mathrm{i}\sqrt{\epsilon/2}\,\mathrm{e}^{\mathrm{i}x}).$$

Here, we calculate that $u(x)$ has winding number π.

We remark that some Hamiltonian systems may have more complicated variations in eigenfunction pairings; one example is $V(x) = \cos^2 x + \mathrm{i}\epsilon\sin^3(2x)$. The restrictions placed on winding number by complex conjugacy pairings, coupled with the absence of nodes, helps to explain their more nuanced behaviors.

2.3. Cubic nonlinearity

Many $\mathcal{PT}$-symmetric nonlinear Schrödinger equations exhibit similar characteristics to their linear counterparts. Let us first examine a Schrödinger equation with an additive *Kerr*, or cubic ($|\psi|^2\psi$), nonlinearity

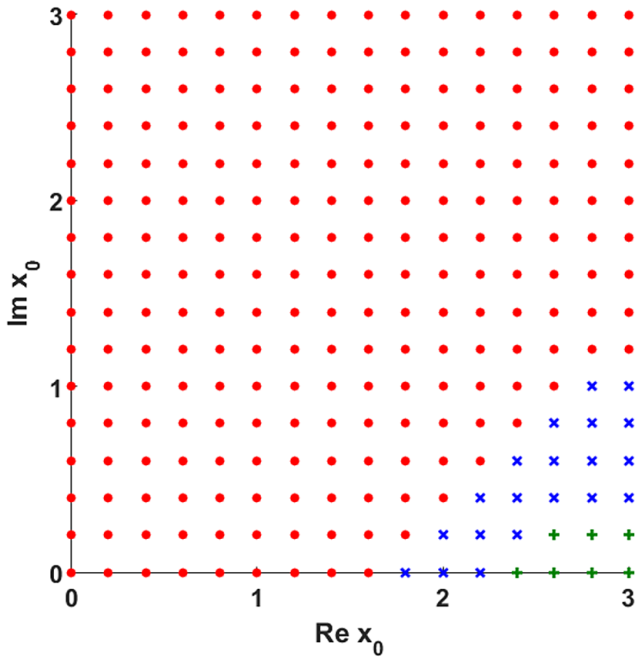

Figure 6. Selected complex initial conditions and the winding numbers to which they give rise for (6). A red dot indicates a winding of π, a blue x indicates a winding of 3π, and a green $+$ indicates a winding 5π. It appears that adjacent regions are separated by a curve of initial conditions, which give rise to separatrix solutions.

$$E\psi(x) = -\psi_{xx}(x) + V(x)\psi(x) + |\psi(x)|^2\psi.$$

This equation is isomorphic to the nonlinear paraxial wave equation governing the propagation of intense light through a waveguide. For figure 5, we analyze the extended stationary states of a periodic potential (5) [20–23]. To find these states we choose a wave intensity

$$P_{\rm uc} = \int \mathrm{d}x|\psi(x)|^2$$

over the unit cell. The value of $P_{\rm uc}$ determines the reality or complexity of the band structure [23]. Thus, adjustment of the parameters $P_{\rm uc}$ and E allows us to change the degree of symmetry breaking present at each part of the spectrum. Singular points correspond to jumps in winding in a manner similar to the linear case. This type of eigenfunction winding evolution occurs regardless of the variable ($P_{\rm uc}$, k, or ϵ) by which we approach an exceptional point.

If we perform the same procedure with the nonintegrable Schrödinger system with quintic nonlinearity

$$E\psi(x) = -\psi_{xx}(x) + V(x)\psi(x) + |\psi(x)|^4\psi(x),$$

using the potential in (5), we again find that the eigenfunction windings appear to be well ordered as in the linear and cubic-nonlinear cases.

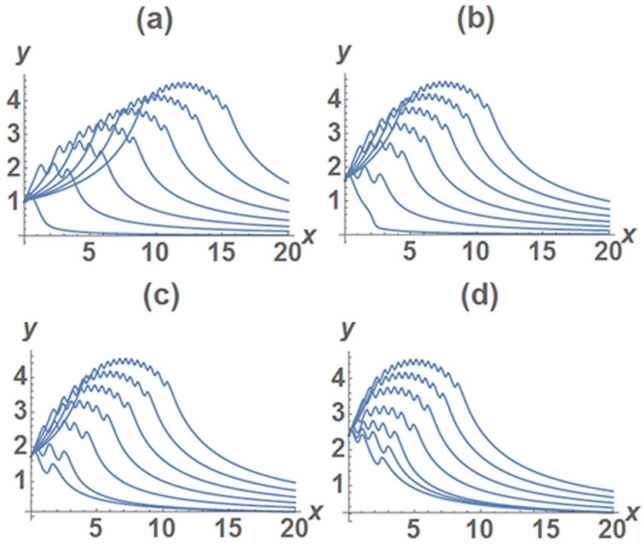

Figure 7. First seven eigenfunctions of the extended cosine problem $y'(x) = \cos[-2\pi n y(x)/\epsilon]$ initial conditions $y'(0) = \epsilon$ and $y'(0) = 1$ for $\epsilon = 1.0, 1.6, 1.7, 2.4$ in panels (a)–(d). On the interval $[0, \infty)$, these eigenfunctions have $(4n + 1)$ extrema, the degenerate signature of winding number $(2n + 1)\pi$. At each exceptional point, one or multiple eigenfunctions each gain two local extrema, or π, of winding.

2.4. Time-dependent systems

One might be tempted to question the utility of using the topological description of eigenfunctions over nodal interlacing. When examining a simple ordinary differential equation system, one need only extend a set of winding eigenfunctions into the complex plane to see the vaguely interlacing-like patterns first described in [11].

However, non-Hermitian, and in particular $\mathcal{PT}$-symmetric systems, are most notable not for their purely mathematical intricacies, but rather for their extensive physical applications. When performing an experiment or computationally modeling a process, one generally has easy access to neither closed-form solutions of waves nor their extensions into the complex plane. We propose that the winding number may prove to provide a convenient metric for classifying these systems and their behaviors.

For example, certain $\mathcal{PT}$-symmetric systems in optics, such as the nonlinear paraxial wave equation, support the propagation of waves stably oscillating in power [23]. When one analyzes a nonlinear extended state described in [23] at each point along its direction of propagation, one finds that changes in winding number correspond to local extrema in its power spectrum. Instead of merely classifying the effective degree of symmetry breaking of the system based on the power of the wave, we may also now classify the effective degree of symmetry breaking intrinsic in the eigenfunction based on its winding number. The combination of these two classifications helps more thoroughly elucidate the regions of wave propagation for each extended state [24]. It is of interest to explore further the connections between winding, propagation dynamics, and stability in physical partial-differential-equation systems.

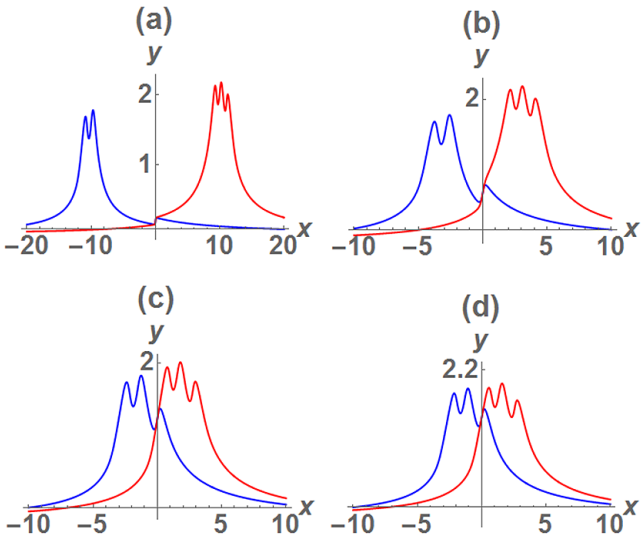

Figure 8. Solutions to $y'_{\pm}(x) = \cos[\pi(x \pm 2\epsilon)y_{\pm}(x)]$ for $\epsilon = 0.5, 0.7, 1.3, 1.5$ for panels (a)–(d). As ϵ increases, $y_{+}(x)$ (red solid curve) and $y_{-}(x)$ (blue dashed curve) pair up and approach translations of one another along the x-axis, similar to the pairing of eigenfunctions in $\mathcal{PT}$ -symmetric Schrödinger systems.

3. Winding interpretation of an initial-value problem

Does function ordering based on topological properties occur outside of Schrödinger models? It is known that a number of other differential equations exhibit interlacing-like oscillatory behaviors, such as the Painlevé transcendents [25] and the much broader classes of Painlevé-like equations described in [26]. In this section we consider one such nonlinear first-order *initial-value problem*

$$y'(x) = \cos[\pi x y(x)], \quad y(0) = a. \tag{6}$$

The solutions to this non-Sturm–Liouville problem for real a on the interval $[0, \infty)$ were described in [27]. The solutions exhibit oscillations that look strikingly similar to the interlacing properties of Sturm–Liouville systems. All solution curves with initial conditions in a range $a_n < a < a_{n+1}$ exhibit the same number of up-and-down oscillations. The values $..., a_{-1}, a_0, a_1, ...a_n, ...$ correspond to separatrix solutions with oscillation number intermediate between the solutions with initial condition on either side. We find that these oscillations wind in the complex plane.

3.1. Winding dependence on the initial y condition

If we perturb the initial condition a into the complex plane, $y(x)$ winds in the space $[x, \mathrm{Re}\, y(x), \mathrm{Im}\, y(x)]$, though not about the axis $x = 0$. The winding number of $y(x)$ on the interval $[0, \infty)$ is dependent on the initial condition a. Initial conditions within specific two-dimensional regions of complex initial condition space all induce the same winding number. These regions appear to be separated by curves of initial conditions inducing separatrix-like behavior (see figure 6).

3.2. Winding dependence on the initial x condition

Let us take (6) with initial condition $y(b) = a$, with b not necessarily zero. We simplify notation by shifting the equation to get

$$y'(x) = \cos[\pi(x-b)(y-a)], \quad y(0) = 0. \tag{7}$$

When we impose $y'(0) = 1$, a condition that always holds for (6), we find that b may take on only a countably infinite number of values $b_n = 2n/a$. We denote the solution corresponding to parameter b_n as $y_n(x)$.

We now examine a set of $y_n(x)$ for positive n. If a is suitably small, we find that solution curves have well-ordered winding numbers on the interval $[0, \infty)$. As we increase a, the winding numbers of one or multiple $y_n(x)$ exhibit sudden shifts (see figure 7). The initial condition b_n acts in a topologically-similar manner to an eigenvalue in a Schrödinger equation, and a behaves similarly to the exceptional-point parameter ϵ. Because (6) lacks nodal interlacing, these parallels only become apparent when we perturb these initial conditions into the complex plane and observe winding.

Therefore, (6) behaves like a precise first-order differential equation model with an exceptional-point parameter or, alternatively, like the lowest eigenfunction of a much broader set of differential equations. In this context the asymptotic calculations presented in [27] mimic the calculation of exceptional point, or operator singularity, locations. We thus see that the construction of a differential equation or its parametrization may affect the perceived topology of solutions. The careful addition of extra parameters or perturbation into the complex plane may enhance our understanding of the nature of eigenfunctions and the origin of winding phenomena.

Now, let us return to (7) and consider negative-n states. On $[0, \infty)$ for $a = 0$, each solution has only one local extremum. That is, for complex a, $W[y_{-n}(x)] = \pi$ for all n. However, as we increase a, the negative-n solutions develop extra oscillations (winds) two at a time, just as the positive-n solutions do. When we broaden our outlook to the full real domain, we notice a pairing phenomenon similar to that of $\mathcal{PT}$-symmetric systems (see figure 8). While $y_n(x)$ and $y_{-n}(x)$ may differ in winding number at $a = 0$, as a increases, they eventually pair off: possessing the same oscillation number and approaching translations of one another along the x-axis. These properties beg whether there exist other general mathematical features to distinguish negative-n solutions from one another prior to the crossing of singular points in the parameter a.

4. Conclusions and outlook

To understand the interlacing of Sturm–Liouville systems, we have shown that it is useful to extend the system into the complex plane. We have done so. This ties together the Sturm–Picone and Sturm Separation Theorems and offers insights into the connections between Hermitian and unbroken $\mathcal{PT}$-symmetric systems.

Winding properties are not restricted to linear systems. We have demonstrated winding in the stationary states of a Schrödinger system with cubic nonlinearity. Winding also helps characterize propagation dynamics and stability in time-dependent systems. We have described how a nonlinear first-order initial-value problem that has interlacing-like behaviors on the real line exhibits winding in the complex plane. A similar analysis should be fruitful for much broader classes of nonlinear systems, such as the Painlevé transcendents. Based on the research presented here, we believe that winding behavior is universal. It is of interest to

probe further the mathematical origin of winding properties and their potential ramifications for experiments.

Acknowledgments

STS thanks H Herzig Sheinfux, Y Lumer, and M Segev for helpful discussions and assistance. Figures were generated using MATLAB and Mathematica.

ORCID iDs

Carl M Bender https://orcid.org/0000-0002-3840-1155

References

[1] Guo A, Salamo G J, Duchesne D, Morandotti R, Volatier-Ravat M, Aimez V, Siviloglou G A and Christodoulides D N 2009 *Phys. Rev. Lett.* **103** 093902
[2] Rüter C E, Makris K G, El-Ganainy R, Christodoulides D N, Segev M and Kip D 2010 *Nat. Phys.* **6** 192
[3] Lin Z, Ramezani H, Eichelkraut T, Kottos T, Cao H and Christodoulides D N 2011 *Phys. Rev. Lett.* **106** 213901
[4] Regensberger A, Bersch C, Miri M-A, Onishchukov G and Christodoulides D N 2012 *Nature* **488** 167
[5] Chtchelkatchev N, Golubov A, Baturina T and Vinokur V 2012 *Phys. Rev. Lett.* **109** 150405
[6] Feng L, Xu Y-L, Fegadolli W S, Lu M-H, Oliveira J E B, Almeida V R, Chen Y-F and Scherer A 2013 *Nat. Mater.* **12** 108
[7] Bender C M 2007 *Rep. Prog. Phys.* **70** 947
[8] Bender C M and Boettcher S 1998 *Phys. Rev. Lett.* **80** 5243
[9] Courant R and Hilbert D 1953 *Methods of Mathematical Physics* I (New York: Interscience) ch 6
[10] Weigert S 2003 *Phys. Rev.* A **68** 062111
[11] Bender C M, Boettcher S and Savage V M 2000 *J. Math. Phys.* **41** 6381
[12] Bender C M and Orszag S A 1978 *Advanced Mathematical Methods for Scientists and Engineers* (New York: McGraw-Hill)
[13] Artin E 1947 *Ann. Math.* **48** 101
[14] Znojil M and Lévai G 2000 *Phys. Lett.* A **271** 377
[15] Gómez-Ullate D, Grandati Y and Milson R 2014 *J. Phys. A: Math. Theor.* **47** 015203
[16] Driver K and Duren P 2001 *Constr. Approx.* **17** 169
[17] Kato T 1966 *Perturbation Theory for Linear Operators* (Berlin: Springer) ch 2
[18] Bender C M and Wu T T 1969 *Phys. Rev.* **184** 1231
[19] Nixon S, Ge L and Yang J 2012 *Phys. Rev.* A **85** 023822
[20] Cohen O, Schwartz T, Fleischer J E, Segev M and Christodoulides D N 2003 *Phys. Rev. Lett.* **91** 113901
[21] Buljan H, Cohen O, Fleischer J W, Schwartz T, Musslimani Z H, Efremidis N K and Christodoulides D N 2004 *Phys. Rev. Lett.* **92** 223901
[22] Jablan M, Buljan H, Manela O, Bartal G and Segev M 2007 *Opt. Express* **15** 4623
[23] Lumer Y, Plotnik Y, Rechtsman M C and Segev M 2013 *Phys. Rev. Lett.* **111** 263901
[24] Schindler S T, Lumer Y, Sheinfux H H and Segev M in progress
[25] Bender C M and Komijani J 2015 *J. Phys. A: Math. Theor.* **48** 475202
[26] Bender C M 2017 *J. Phys.: Conf. Ser.* **873** 012002
[27] Bender C M, Fring A and Komijani J 2014 *J. Phys. A: Math. Theor.* **47** 235204